Proceedings of the International Conference on Oxide Materials for Electronic Engineering, May 29–June 2, 2017, Lviv

Comparison of the Luminescent Properties of $Y_3Al_5O_{12}$:Pr Crystals and Films

T. Zorenko[a,b,*], V. Gorbenko[a,b], S. Nizankovskiy[c] and Yu. Zorenko[a,b]

[a]Institute of Physics, Kazimierz Wielki University in Bydgoszcz, 85-090 Bydgoszcz, Poland

[b]Electronics Department, Ivan Franko National University of Lviv, 79017 Lviv, Ukraine

[c]Institute for Single Crystals, National Academy of Sciences of Ukraine, 61001 Kharkiv, Ukraine

The work is dedicated to comparative investigation of the luminescent properties of $Y_3Al_5O_{12}$:Pr (YAG:Pr) single crystals and single crystalline films using excitation by synchrotron radiation with an energy of 3.7–25 eV in the exciton range of YAG host. We have found that the differences in the excitation spectra and luminescence decay kinetics of YAG:Pr crystals and films are caused by involving the Y_{Al} antisite defects and oxygen vacancies in the crystals and Pb^{2+} flux related dopants in the films in the excitation processes of the Pr^{3+} luminescence. Taking into account these differences, we have determined in more detail the energy structure of the Pr^{3+} ions in YAG host and estimated the differences in the energies of creation of the excitons bound with the isolated Pr^{3+} ions in YAG:Pr films and the dipole Pr–Y_{Al} antisite defect centers in the crystal counterpart.

DOI: 10.12693/APhysPolA.133.948

PACS/topics: 78.55.Hx

1. Introduction

Single crystals (SC) and single crystalline film (SCF) Pr-doped $Y_3Al_5O_{12}$ garnet (YAG:Pr), apart from the application as laser media [1], attract also attention for creating cathodoluminescent screens [2] and scintillators for 2D/3D microimaging with using X-ray or synchrotron (SR) radiation [3]. Meanwhile, the properties of this material in such different crystalline forms are strongly influenced by the differences in the methods and conditions of their preparation.

The luminescence of YAG:Pr garnet has already been investigated in the SC, ceramic and powder states using the traditional spectral methods [1, 2, 4–6] and SR excitation [7, 8]. The luminescent and scintillation properties of the YAG:Pr SCFs have been also investigated by some of us and compared with those of reference SCs using the absorption, cathode- and photoluminescence as well as light yield (LY) measurements under α-particles excitation [9, 10]. We have found that the emission spectra and decay kinetics of YAG:Pr SCF caused by the $5d$–$4f$ transitions of Pr^{3+} ions differ from those for SC counterpart due to (i) the presence of Y_{Al} antisite defects (AD) as emission centers in the UV range and trapping centers in the case of SCs, grown from the melt at high temperatures, (ii) the influence of Pb^{2+} flux related dopants in the case of YAG:Pr SCFs, grown from PbO based flux at significantly lower ($\approx 1000\,^{\circ}C$) temperatures. At the same time, several important questions related to the correct explanation of the observed differences in the luminescent properties of YAG:Pr SCs and SCFs remain unclear up to now and cannot be investigated using the traditional spectral methods.

As a continuation of this direction of research, the aim of the present work is to compare the luminescent properties of YAG:Pr SCs and SCFs using SR excitation in the fundamental absorption range of YAG host. Such a type of excitation enables one to correctly compare the luminescence of YAG matrix in the SCF and SC forms as well as to investigate the luminescent properties of different dopants in them [11–13]. Recently we have successfully performed the detailed comparison of the properties of undoped [11] and Ce^{3+} doped YAG SCs and SCFs [12, 13]. In this work, we pay our attention to the peculiarities of the Pr^{3+} luminescence in the SCs and SCFs of this garnet.

2. Samples under study and experimental technique

The YAG:Pr SCs were grown by the horizontal direct crystallization (HDC) method under Ar atmosphere at the temperature around $2000\,^{\circ}C$ [14]. The YAG:Pr SCFs were prepared by the liquid phase epitaxy (LPE) method from the melt-solutions based on PbO-B_2O_2 flux in air atmosphere onto YAG substrates with (110) orientation at temperatures 960–$1020\,^{\circ}C$ (see [7, 8] for details). For both technologies the same raw materials of 4N (Al_2O_3) and 5N (Y_2O_3 and Pr_4O_7) purity were used.

Comparison of the luminescent properties of YAG:Pr SC and SCF samples was performed using the time-resolved emission spectroscopy of under excitation by SR with an energy of 3.7–25 eV at the Superlumi station at HASYLAB at DESY at 300 K and 10 K. The emission and excitation spectra were measured with a monochromator ARC and PMT Hamamatsu R6358P in both the integral regime and the 1.2–12 ns, 150–200 ns time intervals (fast and slow components, respectively) in the limits of SR pulse with a repetition time of 200 ns. The

*corresponding author; e-mail: tzorenko@ukw.edu.pl

decay kinetics of the luminescence was measured in the 0–200 ns time range. The excitation spectra were corrected for the spectral dependence and intensity of the excitation energy; the emission spectra were not corrected.

3. Experimental results

The luminescence spectra of YAG:Pr SCs and SCFs under excitation by SR with different energies at 300 K and 10 K are presented in Figs. 1 and 2, respectively. From comparison of the emission spectra of YAG:Pr SC and SCF we have exactly determined the structure of the luminescence bands in the UV and visible ranges, related to the d–f and f–f transitions of Pr^{3+} ions, respectively, and the luminescence of defect centers. Generally, the luminescence of YAG:Pr SC in the UV range is the superposition of the self-trapped exciton (STE) emission in the band peaked at 260 nm [9, 10], the d–f luminescence of Pr^{3+} ions in the 300–460 nm range [1, 2] and the luminescence of Y_{Al} antisite defected related centers [9, 10]. Specifically, the luminescence of antisite defect related centers consists of the emission of excitons localized around Y_{Al} AD (LE(AD) centers) in the band peaked at 290 nm and the luminescence of excitons bound with Y_{Al} in the band peaked approximately at 330 nm [9] (Fig. 1b, curves 1 and 2). The luminescence of the last centers dominates in the room temperature range under excitation above the YAG band gap (7.85 eV at 8 K) and causes the visible shift of emission spectra YAG:Pr SCs at 300 K with respect to the spectra at 10 K (Fig. 1a, curves 2 and 1, respectively). Due to the luminescence of LE(AD) and Y_{Al} AD centers, the emission spectra of YAG:Pr SCs do not coincide in the case of excitation with the energies of creation of the excitons bound with Pr^{3+} ions and in the case of excitation in the onset of interband transitions (Fig. 1b, curves 1 and 2, respectively).

As opposed to SC, due to the absence of Y_{Al} AD as emission centers in LPE grown SCF sample, the luminescence spectra of YAG:Pr SCF counterpart keep well the form and position of Pr^{3+} related bands at all excitation energies at 300 K (Fig. 2a, curves 1 and 2) and at 10 K as well (Fig. 2a, curves 1 and 2) taking into account the usual temperature shift (Fig. 2a).

It is important to note that the emission spectra of YAG:Pr SCF, under excitation in the $4f$–$5d$ absorption band (Fig. 2a, curve 2) show the dominant broad d–f emission in the UV range while under excitation with the energy above the YAG host or excitation in the exciton range these spectra show very large contribution of the f–f luminescence in the visible range (Fig. 2a, curve 1). The observed f–f emission can originate at the $^3P_0$ level which under the $4f$–$5d$ excitation can be reached by the $4f5d \rightarrow {}^3P_J$ and/or $^1I_6$ radiative transitions followed by the non-radiative relaxation to the $^3P_0$ level. In the case of the YAG host excitation, the energy can be reached to the $5d$ levels and simultaneously also directly transferred to the ^3P_J or $^1I_6$ levels of the Pr^{3+} ion.

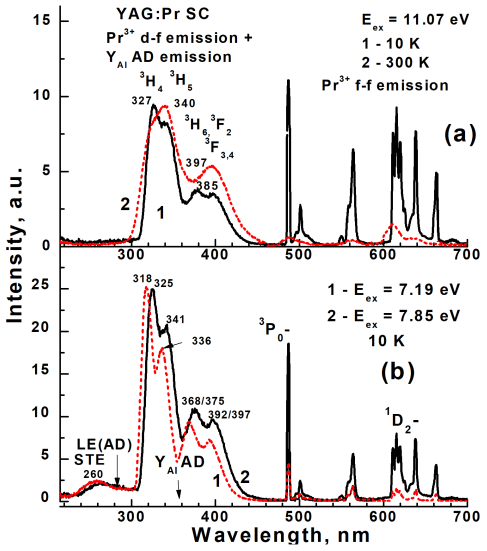

Fig. 1. Emission spectra of YAG:Pr SC at 300 K (a) and 10 K (a,b) under excitation by SR in the range of interband transitions (1a, 2a), at the onset of interband transitions (2b) and with the energies of creation of excitons bound with Pr^{3+} ions (1b). Positions of STE emission band and bands related to Y_{Al} AD are indicated.

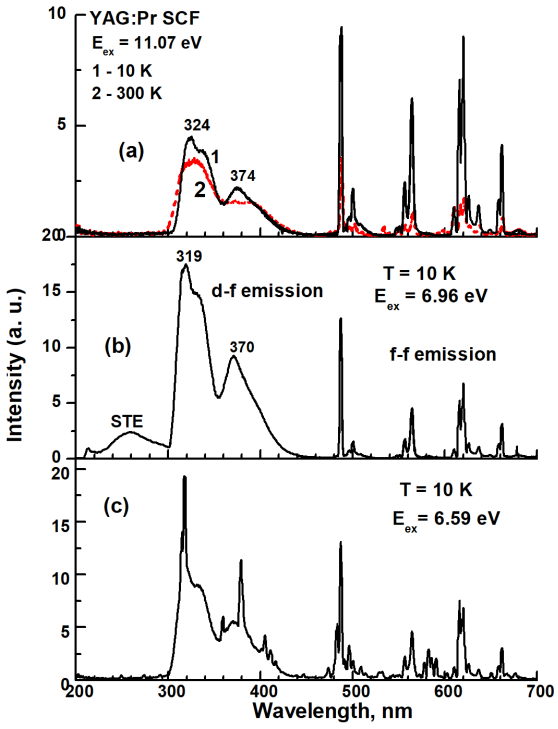

Fig. 2. Emission spectra of YAG:Pr SCF at 300 K (a) and 10 K (a)–(c) under excitation by SR with energy of 11.07 eV above YAG band gap (1a), with an energy of 6.94 eV in the range of creation of excitons bound with Pr^{3+} ions (b) and with an energy of 6.59 eV in the range of $4f5d$ transitions (c).

The excitation spectra of the Pr^{3+} d–f luminescence in YAG:Pr SC and SCF, registered at 320 nm in the different time intervals, are presented in Fig. 3a and 4a, respectively. In the transmittance range of YAG host (3.7–6.5 eV) these spectra consist of the two strong doublet bands with peaks at 4.16 and 4.45 eV and 4.93–5.25 eV, related to $4f$–$5d$ (E_1 and E_2) transitions of Pr^{3+} ions, as well as the unresolved band peaked at 6.17 eV, most probably related to the $4f$–$5d$ (T_{2g}) transitions of Pr^{3+} ions. The structure of the mentioned doublet bands was attributed in [8] to the transitions between $^3H_4$ ground level of $4f^2$ state and two low-spin (LS) and high-spin (HS) levels of $4f$–$5d$ (E_1 and E_2) bands of the $4f5d$ configuration of the Pr^{3+} ion. Usually the excitation spectra of the Pr^{3+} doped YAG SC are highly distorted in the case of relatively high Pr concentration at which the well-known phenomenon of saturation of the high intensity peaks occurs (Fig. 3a). For this reason, the separation of the LS and HS of $4f5d(E_1)$ and $4f5d(E_2)$ bands is more clearly evident in the excitation spectra of the Pr^{3+} luminescence in YAG:Pr SCF (Fig. 4a).

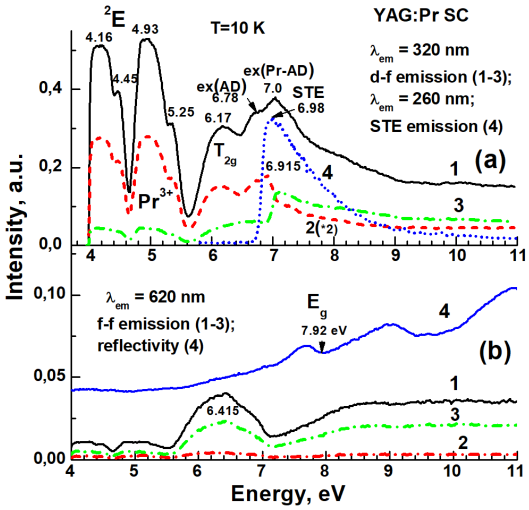

Fig. 3. Excitation spectra of integral (1.2–200 ns, curves 1) (1), fast (1.2–12 ns, curves 2) and slow (150–200 ns, curves 3) components of Pr^{3+} d–f luminescence at 310 nm (a) and Pr^{3+} f–f luminescence at 610 nm (b) in YAG:Pr SC at 10 K. Excitation spectrum of STE luminescence in YAG:Pr SC is shown also for comparison (curve 4b). Curve 4b — reflectivity spectrum of YAG:Pr SC. Curve 2a is multiplied by a factor of 2. E_g is the band gap value of YAG host at 10 K.

Taking into account the position of the low energy excitation bands (Fig. 4a) and the high-energy emission band of Pr^{3+} ions (Fig. 2b) at 10 K, we can also estimate the Stokes shift of the Pr^{3+} luminescence in YAG:Pr host which is equal to 0.385 eV. This value is in good agreement with the data presented in [15].

The excitation spectra of the intrinsic and Pr^{3+} luminescence in YAG:Pr SC and SCF in the exciton range and at the onset of interband transitions are presented

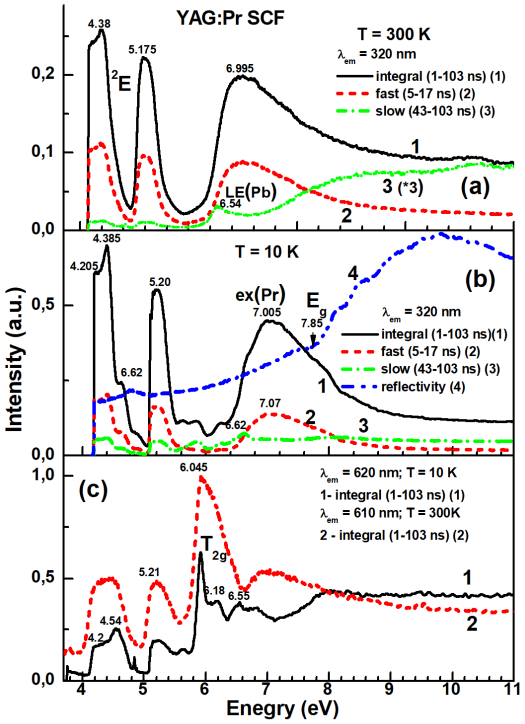

Fig. 4. Excitation spectra of integral (1–103 ns, curves 1) (1), fast (5–17 ns, curves 2) and slow (43–103 ns, curves 3) components of Pr^{3+} d–f luminescence at 310 nm (a) and Pr^{3+} f–f luminescence at 610 nm (b) in YAG:Pr SCF at 300 K (a) and 10 K (b,c). Curve 3a is multiplied by a factor of 3. Curve 4b — reflectivity spectrum of YAG:Pr SCF.

in Figs. 3 and 4, respectively. The main excitation band of the STE luminescence in YAG SC is peaked at 7.15 eV [12, 13] (Fig. 3a, curve 4). Excitation spectra of the fast component of the Pr^{3+} luminescence in YAG:Pr garnet in the 6.5–11 eV range consist of the dominant bands peaked at different energies, namely, at 6.915 eV in SC (Fig. 3a, curve 2) and at 7.005 eV in SCF (Fig. 4a, curve 2). The mentioned excitation energies correspond to the energy of creation of excitons bound with isolated Pr^{3+} ions in SCF and most probably with dimer Pr^{3+}-AD centers in SC [12].

The bump at 6.78 eV in the excitation spectra of the integral and slow component of Pr^{3+} luminescence in YAG:Pr SC can correspond to the energy of creation of excitons localized around Y_{Al} centers emitting in the 280 nm band (see [12, 13] for details). Excitation of this AD related emission band, located in the range of the $4f5d(E_1)$ Pr^{3+} absorption band, results also in the excitation of the Pr^{3+} luminescence. Due to relatively slow emission of AD centers with decay time in the hundred ns range [12, 13], such process causes also the large content of slow component in the Pr^{3+} luminescence (Fig. 3a, curve 3). As opposed to SCs, the small bump at 6.62 eV in the excitation spectra of YAG:Pr SCF (Fig. 4a,

curve 1) most probably have another nature and can relate to the creation of excitons localized around Pb^{2+} centers [13]. At the same time, it is important to note here that intensity of slow component of the Pr^{3+} luminescence is significantly (by one order of the magnitude) lower in the YAG:Pr SCF (Fig. 4a, curve 3) than that in the SC counterpart (Fig. 3a, curve 3).

Therefore, the notable differences are observed in the excitation spectra of YAG:Pr SC and SCF which are caused by involving the Y_{Al} ADs in SCs and Pb^{2+} flux related dopants in SCFs in the excitation processes of the Pr^{3+} luminescence in YAG hosts. Namely, we have observed the 0.009 eV difference in the energies of creation of the excitons bound with the isolated Pr^{3+} ions in YAG:Pr SCF (Fig. 4a, curve 2) and dipole Pr–Y_{Al} AD centers in the SC counterpart (Fig. 3a, curve 2). Based on the excitation and reflection spectra of YAG:Pr SC and SCF we can also estimate the YAG band gap value of 7.85 eV at 10 K and relative positions of the Pr^{3+} $5d$ levels in LuAG band structure.

The excitation spectra of the f–f luminescence in YAG:Pr SC and SCF registered at 610 nm are presented in Fig. 3b and 4b, respectively. From the excitation spectra of the f–f luminescence in YAG:Pr SC and SCF we have observed that: (i) the exciton-like excitation bands are not observed for this emission, (ii) f–f emission is excited mainly in the broad complex bands peaked correspondingly at 6.415 eV in SC (Fig. 3b, curve 1) and at 6.15 eV with bump at 6.045 eV in SCFs (Fig. 4b, curves 1). The last band well coincides with the $4f$–$5d$ (T_{2g}) transitions of Pr^{3+} ions. Therefore, we can conclude that the f–f luminescence of Pr^{3+} ions is well excited by the d–f luminescence (Fig. 3b and 4b). The relatively larger contributions of the $4f$–$4f$ emission under excitation to the exciton range and $4f5d(T_{2g})$ bands indicate the involvement of the Pr^{3+} bound exciton in the energy transfer to Pr^{3+} $4f5d(T_{2g})$ states and 4f(^3P_J, $^1I_6$) levels. In this case the relatively large distance lattice relaxation of the Pr^{3+} bound exciton results in the high population of the $^3P_0$ level and the intensive f–f luminescence.

The comparison of the luminescence decay kinetics of YAG:Pr SC and SCF is presented in Fig. 5a and Fig. 6a at 300 K as well as in Fig. 5b and 6b at 10 K. Under excitation in the intrinsic Pr^{3+} excitation bands at 4.42 eV at 10 K and 300 K, the decay curves of the Pr^{3+} luminescence in YAG:Pr SCF can be characterized by decay times of 16.5 ns and 10.5 ns (Fig. 6, curves 3b and 3a, respectively). We have also found the notable differences in the decay kinetics of YAG:Pr SCFs and SCs under high energy excitation (Fig. 5a and 6a, curves 1) and excitation in the exciton range (Fig. 5a and 6a, curves 2). These differences are caused by participation of the ADs in SC and Pb^{2+} flux related dopant in SCF in the excitation processes of the Pr^{3+} luminescence in YAG host as emission centers and trapping centers as well. In such a way the delivery of the excitation energy to the emission centers can be significantly delayed in YAG:Pr SCF and SC. Namely, due to excitation of the Pr^{3+} luminescence in YAG:Pr SC by the emission of Y_{Al}AD related centers (Fig. 3a) as well as the temporal localization of charge carriers at these centers [16], the decay kinetics of the Pr^{3+} luminescence in SC is notable slower (Fig. 5a and b, curves 1) than that in SCF analogue (Fig. 6a and b, curves 1). On the contrary, under excitation in the range of interband transitions and exciton range, the decay kinetics of the Pr^{3+} luminescence in YAG:Pr SCF is notably faster both at 300 K and 10 K (Fig. 6a and b, curves 1 and 2) due to the absence of Y_{Al} ADs and lower concentration of oxygen vacancies. Specifically, under high-energy excitation (10.5–15 eV) the average decay time of the Pr^{3+} luminescence in YAG:Pr SCF at 300 K and 10 K is equal to 26 and 27.5 ns, respectively.

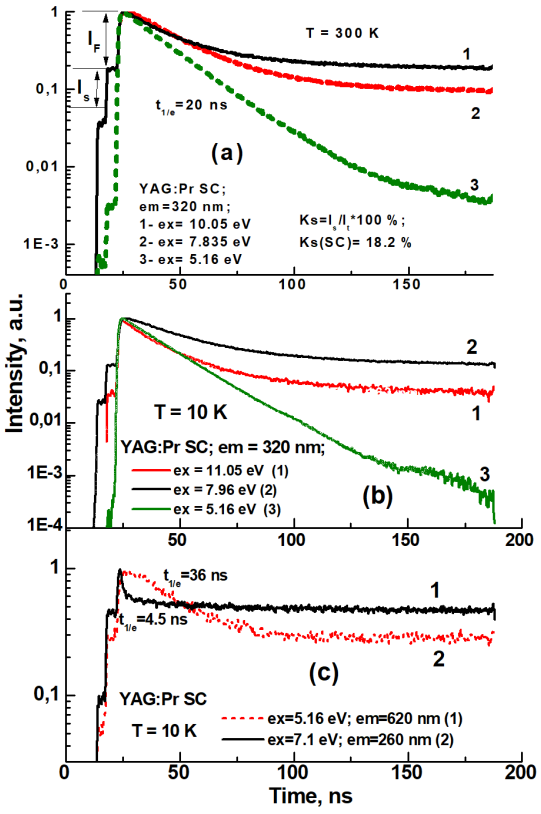

Fig. 5. Comparison of decay kinetics of Pr^{3+} d–f luminescence in 305–320 nm range in YAG:Pr SC at 300 K (a) and 10 K (b) in the range of interband transitions of YAG host (curves 1a and 1b); under in the exciton range (2a and 2b) and excitation in the Pr^{3+} absorption bands (3a and 3b); (c) decay kinetics of Pr^{3+} f–f luminescence at 610 nm at 10 K under excitation in the exciton range of YAG host (c1) and in the range of Pr^{3+} absorption band (c2). The decay kinetics of STE luminescence in YAG:Pr SC (Fig. 5c, curve 2).

We have also estimated the content of the slow components in the decay of the YAG:Pr SC and SCF under high-energy (10.05–15 eV) excitation, using the ratio between intensity I_s of the decay components, which is slower than the repetition frequency of SR (200 ns) and

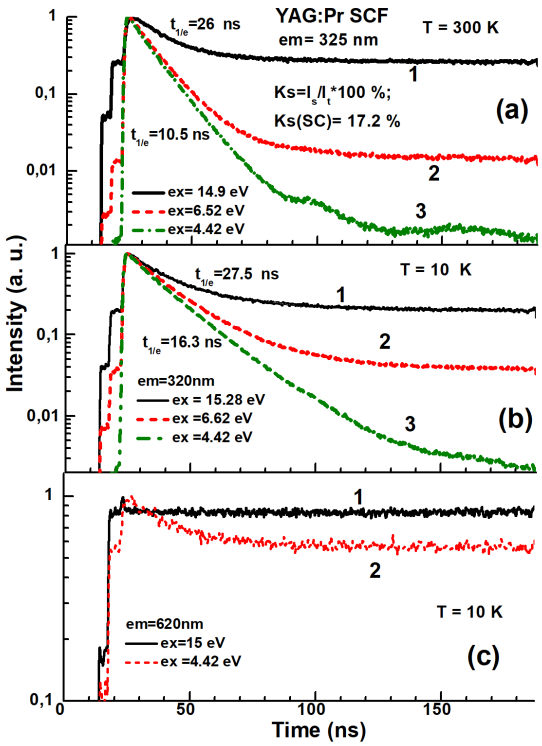

Fig. 6. Comparison of decay kinetics of Pr^{3+} d–f luminescence in 320–325 nm range in YAG:Pr SCF at 300 K (a) and 10 K (b) in the range of interband transitions of YAG host (curves 1a and 1b); under in the exciton range (2a and 2b) and excitation in the Pr^{3+} absorption bands (3a and 3b); (c) decay kinetics of Pr^{3+} f–f luminescence at 610 nm at 10 K under excitation in the range of interband transitions of YAG host (c1) and in the range of Pr^{3+} absorption band (c2).

the decay amplitude I_t of the rising part of the decay curve as $K_s = [I_s/I_t] \times 100\%$ (Fig. 5a and 6a). The content of slow components is slightly larger in YAG:Pr SCs (18.2%) than that in SCF (15.2 %) (see Fig. 5). The main reason for such a slowing-down of the decay of the Pr^{3+} luminescence and an increase of the amount of slow emission components in YAG:Pr SC, grown at high temperature in reducing atmosphere is the presence of large content of Y_{Al} AD and oxygen vacancies as emission and trapping centers in comparison with the condition of low-temperature crystallization of SCFs from the melt-solution in air.

The decay kinetics of the f–f luminescence in YAG:Pr SC and SCF at 10 K under excitation with an energy in the exciton range or range of interband transition as well as in the $4f5d$ (E_2) absorption band is shown in Fig. 5c and 6c, curves 1 and 2, respectively. The luminescence decay kinetics possesses the fast component with a decay time of 39 ns, corresponding to the excitation of the f–f luminescence via the d–f transitions and the main slow component in the microsecond range which cannot be estimated due to time limitation of the applied setup.

The decay kinetics of the STE luminescence in YAG:Pr SC (Fig. 5c, curve 2) is very close to the previously observed one in undoped YAG SC [12] and is related to the radiative annihilation from single and triplet relaxed state with a decay time of 4.8 ns (for fast component) and with a decay time in hundred ns range (for slow emission component), respectively.

4. Conclusions

Comparison of the luminescent properties of YAG:Pr SC, grown from the high temperature melt by HDC method, and SCF grown by the low temperature LPE method from PbO based flux, was performed using the time-resolved emission spectroscopy under excitation by synchrotron radiation with an energy of 3.7–25 eV at the Superlumi station at HASYLAB at DESY at 300 K and 10 K.

Based on the obtained results, we have more exactly determined the energy structure of the Pr^{3+} ions in YAG host. We have found the notable differences in the Pr^{3+} luminescence and excitation spectra as well as the luminescence decay kinetics in YAG:Pr SC and SCF caused by involving the Y_{Al} antisite defects (AD) and oxygen vacancies in SCs and Pb^{2+} flux related dopants in SCF in the excitation processes of the Pr^{3+} luminescence in these crystalline forms of the mentioned garnet. We have also estimated the differences in the energies of creation of the excitons most probably bound with the isolated Pr^{3+} ions in YAG:Pr SCFs and dipole Pr-Y_{Al} AD centers in the SC counterpart.

We have also found that the decay kinetics of Pr^{3+} ions is notably influenced by the Pb^{2+} flux related impurity. Meanwhile, under excitation in the range of interband transitions and exciton range, the decay kinetics of the Pr^{3+} luminescence in YAG:Pr SCFs is faster and the content of slow emission component is notably lower than that in YAG:Pr SC counterpart due to the absence of Y_{Al} ADs and lower concentration of oxygen vacancies in the SCF samples in comparison with their SC counterparts.

Acknowledgments

This work was realized within Polish NCN 2016/21/B/ST8/03200 project and partly supported by Ukrainian CE-76 F project. The investigations at the Superlumi station (Hasylab at DESY) were performed within I-20110938 EC project.

References

[1] J. Pejchal, M. Nikl, E. Mihokova, J.A. Mares, A. Yoshikawa, H. Ogino, K.M. Schillemat, A. Krasnikov, A. Vedda, K. Nejezchleb, *J. Phys. D Appl. Phys.* **42**, 10 (2009).

[2] T. Yanagida, Y. Fujimoto, K. Kamada, D. Totsuka, H. Yagi, T. Yanagitani, Y. Futami, S. Yanagida, S. Kurosawa, Y. Yokota, A. Yoshikawa, M. Nikl, *IEEE Trans. Nucl. Sci.* **59**, 2146 (2012).

[3] Yu. Zorenko, V. Gorbenko, T. Voznyak, T. Martin, P.-A. Douissard, J.A. Mares, M. Nikl, *Proc. SPIE* **7310**, 731007 (2009).

[4] J.A. Mares, Y. Shi, M. Nikl, Y. Shen, Y. Pan, X. Feng, *IOP Conf. Series Mater. Sci. Eng.* **15**, 6 (2010).

[5] W. Drozdowski, P. Dorenbos, R. Drozdowska, A.J.J. Bos, N.R.J. Poolton, M. Tonelli, M. Alshourbagyet, *IEEE Trans. Nucl. Sci.* **56**, 320 (2009).

[6] Y. Shi, M. Nikl, X. Feng, J.A. Mares, Y. Shen, A. Beitlerova, R. Kucerkova, Y. Pan, Q. Liu, *J. Appl. Phys.* **109**, 013522 (2011).

[7] J.M. Ogiegło, A. Zych, T. Jüstel, A. Meijerink, C.R. Ronda, *Opt. Mater.* **35**, 322 (2013).

[8] A. Wojtowicz, K. Brylew, M.E. Witkowski, W. Drozdowski, K. Kamada, T. Yanagida, A. Yoshikawa, *Hasylab Annual Report*, 2012, p. 2.

[9] V. Gorbenko, Yu. Zorenko, V. Savchyn, T. Zorenko, T. Zorenko, A. Pedan, V. Shkliarskyi, *Radiat. Measur.* **45**, 461 (2010).

[10] V. Babin, V. Gorbenko, A. Krasnikov, A. Makhov, M. Nikl, S. Zazubovich, Yu. Zorenko, *Radiat. Measur.* **45**, 415 (2010).

[11] Yu. Zorenko, A. Voloshinovskii, V. Savchyn, T. Vozniak, M. Nikl, K. Nejezchleb, V. Mikhailin, V. Kolobanov, D. Spassky, *Phys. Status Solidi B* **244**, 2180 (2007).

[12] Y. Zorenko, V. Gorbenko, E. Mihokova, M. Nikl, K. Nejezchleb, A. Vedda, V. Kolobanov, D. Spassky, *Radiat. Measur.* **42**, 521 (2007).

[13] Yu. Zorenko, T. Voznyak, V. Gorbenko, T. Zorenko, A. Voloshinovski, V. Vistovsky, M. Nikl, K. Nejezchleb, V. Kolobanov, D. Spasski, *Opt. Spectrosc.* **104**, 75 (2008).

[14] S.V. Nizhankovsky, A.Ya. Dan'ko, Yu.V. Zorenko, V.V. Baranov, L.A. Grin', V.F. Tkachenko, P.V. Mateichenko, *Phys. Solid State* **53**, 127 (2011).

[15] K. Ivanovskikh, J.M. Ogiegło, A. Zych, C.R. Ronda, A. Meijerink, *ECS J. Solid State Sci. Technol.* **2**, R3148 (2013).

[16] M. Nikl, J. Pejchal, E. Mihokova, J.A. Mares, H. Ogino, A. Yoshikawa, T. Fukuda, A. Vedda, C. D'Ambrosio, *Appl. Phys. Lett.* **88**, 41916 (2006).